

Λ -nucleus single-particle potentials

D. J. Millener and C. B. Dover

Brookhaven National Laboratory, Upton, New York 11973

A. Gal

Racah Institute of Physics, The Hebrew University, Jerusalem 91904, Israel

(Received 6 May 1988)

Data on the level spectra of Λ hypernuclei, obtained from (π^+, K^+) and (K^-, π^-) reaction studies, are analyzed to obtain a density-dependent and nonlocal Λ -nucleus potential. We relate our results to previous work which bears on the origin of the density dependence and nonlocality of the Λ -nucleus potential. We argue that the distinguishable Λ particle provides one of the best examples of single-particle shell structure in nuclear physics.

I. INTRODUCTION

Recently, the energy levels of the strange Λ hyperon bound in heavy nuclear systems have been measured¹ in studies of the (π^+, K^+) associated production reaction with nuclear targets ranging from ${}^9\text{Be}$ to ${}^{89}\text{Y}$. The excitation spectra for the (π^+, K^+) process¹ consist of a series of well-defined peaks which blend into a smoothly rising background for high excitation energy. These peaks can be identified with the various orbital angular momentum states $s_\Lambda, p_\Lambda, d_\Lambda, f_\Lambda, \dots$ of the hyperon. Since the spin-dependent components of the Λ -nucleon (ΛN) effective interaction are known to be small,² the fine structure of the peaks is not resolvable with the typical experimental energy resolution³ of approximately 3 MeV. For the case of ${}^{12}\text{C}(\pi^+, K^+)_{\Lambda}{}^{12}\text{C}$, where the angular distribution $d\sigma/d\Omega$ was measured,⁴ the identification of observed peaks with s_Λ and p_Λ single-particle strength was verified.

Data from emulsion studies provide accurate values for s_Λ binding energies in light nuclei⁵ and upper limits on B_Λ for medium-mass nuclei.⁶ These data can be described by a local Woods-Saxon potential well with a depth of about 30 MeV.⁷ More recently, (K^-, π^-) reactions with low momentum transfer have yielded data on substitutional orbits (l_Λ same as that of a valence neutron orbit) and in some cases on an adjacent orbit via $\Delta L = 1$ transfer. For example, the (K^-, π^-) reaction has been studied for ${}^{32}\text{S}$ and ${}^{40}\text{Ca}$ targets⁸ and for ${}^{12}\text{C}$, ${}^{27}\text{Al}$, ${}^{51}\text{V}$, and ${}^{209}\text{Bi}$ targets.⁹ A Woods-Saxon well with a depth of about 30 MeV again gives a reasonable account of these data.¹⁰ The new (π^+, K^+) data¹ enable us to follow the evolution of Λ binding energies over an appreciable range of nuclear core mass number A and also, in a number of cases, provide us with a complete set of bound and first unbound energy levels for nodeless Λ orbitals at fixed A .

For many years, attention has been paid to the problem of determining the well depth for a Λ particle in nuclear matter.^{7,11} As indicated in the preceding paragraph, this depth, determined from the asymptotic binding energy of the lowest s orbit for large A , is in the vicinity of 30 MeV. With data available on the spacing of single-

particle levels in a given hypernucleus, one can determine a radius parameter in addition to a depth. The next step is to examine the systematics of these parameters as a function of A . It turns out that a Woods-Saxon well, say, of fixed depth with a radius parameter r_0 [$R = r_0(A-1)^{1/3}$] that decreases with A can fit the data on single-particle binding energies.¹² Then, one can try to understand the origin of this potential in terms of a functional dependence on the density of the nuclear core and parameters characterizing the effective ΛN interaction.

In Sec. II we provide a description of the body of binding-energy data in terms of Λ -nucleus potentials motivated by the spherical Skyrme Hartree-Fock approach of Rayet.¹³ There is sufficient flexibility in these potentials through a basic term linear in the density, a repulsive term depending on a higher power of the density, and a nonlocality in the form of an effective mass to describe the data. We compare these potentials with other phenomenological density-dependent potentials. Also, we review progress on the derivation of density-dependent G matrices from the free ΛN interaction and the subsequent construction of a nonlocal and density-dependent Λ -nucleus potential from first principles.

In Sec. III we make a comparison of the Λ -nucleus potential with the corresponding nucleon-nucleus potential. Also, we consider whether the quark substructure of the Λ could manifest itself in an observable way in terms of Fock-type exchange corrections to the Λ mean field due to antisymmetrization of the nonstrange quarks in the Λ with those in neighboring nucleons. A preliminary discussion of this issue, highlighting Λ -nucleus shell spacings, has been given previously.¹² In Sec. IV we summarize our results, discuss recent attempts to construct Λ -nucleus potentials from the free ΛN interaction, and present our conclusions.

II. RESULTS

A. Model for the potential

The observed Λ binding energies B_Λ are shown as a function of $A^{-2/3}$ in Fig. 1. As stated in the Introduction, we consider a description of these results in terms of

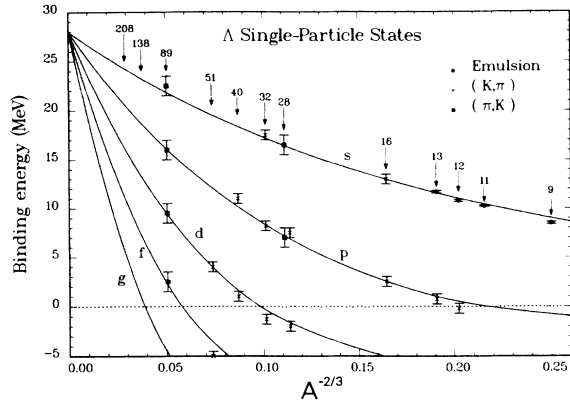


FIG. 1. The data on binding energies (B_Λ) of Λ single-particle states, derived from in-flight (π^+, K^+) and (K^-, π^-) reactions (Refs. 1, 4, 8, and 9) and emulsion data (Ref. 5), as a function of $A^{-2/3}$, where A is the mass number of the core nucleus. The (π^+, K^+) data for $A=9, 12$, and 16 give binding energies in agreement with those from other sources. (π^+, K^+) data has also been taken for $A=40$ and 51 . The curves correspond to the solutions obtained for a Woods-Saxon well with a depth of 28 MeV and a radius parameter $r_0=1.128+0.439A^{-2/3}$. The arrows correspond to various values of the target mass number.

Λ -nucleus potentials of increasing degrees of complexity motivated by the spherical Skyrme Hartree-Fock approach of Rayet.¹³ Following Dover and van Giai,¹⁴ we use an equivalent local potential $V_L(r, E)$ of the approximate form

$$V_L(r, E) = \frac{m^*(r)}{m} U(r) + \left[1 - \frac{m^*(r)}{m} \right] E, \quad (1)$$

$$U(r) = \tilde{t}_0 \rho(r) + \frac{3}{8} t_3 \rho^2(r) + \frac{1}{4} (t_1 + t_2) T(r), \quad (2)$$

$$T(r) = \frac{3}{5} \left(\frac{3}{2} \pi^2 \right)^{2/3} \rho^{5/3}(r), \quad (3)$$

$$\frac{\hbar^2}{2m^*(r)} = \frac{\hbar^2}{2m} + \frac{1}{4} (t_1 + t_2) \rho(r). \quad (4)$$

Here m is the free space Λ mass and $m^*(r)$ is the effective Λ mass in the nuclear medium of density $\rho(r)$. We have set $N=Z$ and neglected derivatives of the density. We shall ultimately use densities which are proportional to the empirically determined charge densities,¹⁵ but for illustrative purposes we will often characterize $\rho(r)$ by a Fermi distribution:

$$\rho(r) = \rho_0 f(r), \quad (5)$$

$$f(r) = (1 + e^{(r-c)/a})^{-1}, \quad (6)$$

$$\rho_0 = \frac{3A}{4\pi c^3} \left[1 + \frac{\pi^2 a^2}{c^2} \right]^{-1}, \quad (7)$$

$$\frac{5}{3} \langle r^2 \rangle = c^2 + \frac{7}{3} \pi^2 a^2. \quad (8)$$

It can be seen from Eqs. (1)–(4) that there are three parameters in the model, \tilde{t}_0 , t_3 , and t_1+t_2 . For smooth densities, such as the Fermi distribution, t_1+t_2 is equivalent, through Eq. (4), to $m^*(0)/m$. The origin of the various terms is discussed in more detail as our pre-

sentation evolves. The standard Skyrme Hartree-Fock parametrization¹⁶ has been retained to facilitate the comparison of Λ -nucleus and nucleon-nucleus potentials.

The approach outlined above uses the basic elements of the Skyrme Hartree-Fock formalism to obtain a physically motivated parametrization of the Λ binding energies in terms of a potential. We identify the Λ binding energies with the eigenenergies of the Schrödinger equation for the potential $V_L(r, E)$. Strictly, B_Λ should be identified¹⁷ with the difference between the total Hartree-Fock energies of the core nucleus and the hypernucleus. Thus, we ignore a rearrangement effect arising from the polarization (contraction or dilation) of the core by the presence of the Λ . However, Rayet¹³ has noted that the polarization of the core vanishes for $t_3 \sim 3000$ MeV fm⁶; the core contracts for smaller t_3 and dilates for larger t_3 . It so happens that the values of t_3 which are required to fit the observed B_Λ values are close to 3000 MeV fm⁶, and the neglect of polarization effects is justified. A term proportional to the center-of-mass kinetic energy, which must be subtracted from the Hartree-Fock energies, also contributes¹⁷ to the rearrangement energy. This correction can be only approximately evaluated, and it is largest for light nuclei where the Hartree-Fock calculation itself is least reliable for the core radii and densities. We use empirical charge densities and neglect all rearrangement corrections in addition to the neglect of derivative terms in the Hartree-Fock potential.

B. Woods-Saxon parametrization of the data

The simplest description of the binding energies is in terms of a local Λ -nucleus potential ($t_1+t_2=0$, $m^*/m=1$) which we write in the simple form

$$-V(r) = V_1 f(r) - V_2 f^2(r), \quad (9)$$

where $c=r_0(A)A^{1/3}$, and V_1 , V_2 , and the diffusivity a are independent of A . The choice $V_1=30.7$ MeV, $V_2=0$, $r_0=1.1$ fm, $a=0.6$ fm was used¹⁸ to predict the A dependence of Λ binding energies (see also Refs. 7 and 10). This model is in substantial agreement with the data. However, the availability of data on the spacing of levels for a given A enables one to fit $r_0(A)$ and V_1 for the simple Woods-Saxon potential with fixed diffusivity (to which there is only a limited sensitivity). One then finds that $r_0(A)$ should decrease slowly with increasing A . For example, in a preliminary fit to the B_Λ values from (π^+, K^+) data, it was found¹² that the choice $V_1=29.34$ MeV, $r_0(A)=(1.080+0.395A^{-2/3})$ fm provides a better description of both light and heavy hypernuclei. In fact, a slightly shallower potential ($V_1=28.0$ MeV) with a larger radius, $r_0(A)=(1.128+0.439A^{-2/3})$ fm, does even better for the data in Fig. 1. The curves in Fig. 1 are calculated for the latter potential.

As will become clear in the next subsection, a potential of the form of Eq. (9), with $V_2=0$ and a constant V_1 , cannot be related directly to the simplest form of $U(r)$ in Eq. (2) with only the $\tilde{t}_0 \rho(r)$ term. Within the approach outlined in Sec. II A, some density dependence or nonlocality is necessary to fit the data.

C. Geometrical considerations

We might expect the term in the potential which is linear in the density to result from the folding of the density-independent part of the ΛN effective interaction with the point nucleon density. The resultant potential well, with $\langle r^2 \rangle = \langle r^2 \rangle_\rho + \langle r^2 \rangle_{\Lambda N}$, is a distribution with increased diffusivity and a slightly smaller half-density radius¹⁹ (see Ref. 20 for examples where the results of folding have been refitted with Fermi functions). Since the longest-range component in the ΛN interaction has a range comparable to the nucleon size, we can take the linear term in Eq. (9) to be proportional to the empirical charge density.¹⁵ Myers¹⁹ has emphasized that the fundamental quantity of geometric importance in describing nuclear densities is the equivalent sharp radius R which scales as $A^{1/3}$. Then it follows that

$$R_{1/2} = R \left[1 - \frac{b^2}{R^2} + \dots \right] \quad (10)$$

and

$$\langle r^2 \rangle^{1/2} = \left[\frac{3}{5} \right]^{1/2} R \left[1 + \frac{5}{2} \frac{b^2}{R^2} + \dots \right], \quad (11)$$

where $R_{1/2}$ is the half-density radius, $\langle r^2 \rangle^{1/2}$ is the rms radius, and b parametrizes the surface thickness. Note that for the Fermi distribution of Eq. (6), we have $R_{1/2} = c$ and $b = \pi a / \sqrt{3}$. Experimental values¹⁵ of $\langle r^2 \rangle^{1/2}$ for the important sequence of target nuclei for (π^+, K^+) reactions (^{16}O , ^{28}Si , ^{51}V , ^{89}Y , ^{138}Ba , ^{208}Pb), with last-filled high-spin neutron orbits,¹⁸ are listed in Table I, together with values obtained from an empirical expression, of the form in Eq. (11), fitted to medium and heavy nuclei.²¹ Also given are values of r_0 , obtained in several ways, for Fermi distributions which reproduce the charge radii under the assumption that $a = 0.54$ fm. It can be seen that these radius parameters behave differently as a function of A and are smaller than those for the potential wells which roughly reproduce the measured Λ binding energies. In fact, the difference between the half-depth radii of the potentials and the charge densities is of the order of 0.5 fm (last row of Table I).

TABLE I. Parametrizations of charge radii (in fm).

A	16	28	51	89	138	208
$r_{\text{ch}}(\text{expt})^a$	2.73	3.10	3.62	4.24	4.84	5.50
$r_{\text{ch}}(\text{fit})^b$	2.74	3.13	3.66	4.28	4.87	5.51
$r_0(\rho)^c$	0.946	1.004	1.049	1.080	1.099	1.116
$r_0(\rho)^d$	0.943	1.006	1.051	1.080	1.096	1.108
$r_0(V)^e$	1.200	1.177	1.160	1.150	1.144	1.140
$\Delta R_{1/2}^f$	0.63	0.51	0.40	0.31	0.25	0.19

^a $r_{\text{ch}} = \langle r^2 \rangle^{1/2}$ is the experimental rms charge radius (Ref. 15).

^b $r_{\text{ch}} = 0.891 A^{1/3} (1 + 1.565 A^{-2/3} - 1.043 A^{-4/3})$ from a fit to experimental charge radii (Ref. 21). Note that $0.891 = 1.15\sqrt{3}/5$ [cf. Eq. (11)].

^cDerived from $r_{\text{ch}}(\text{expt})$ assuming a Fermi distribution with $a = 0.54$ fm for $\rho(r)$.

^d $r_0 = 1.144 - 1.276 A^{-2/3}$, a parametrization of the fit to $r_{\text{ch}}(\text{expt})$.

^e $r_0 = 1.128 + 0.439 (A - 1)^{-2/3}$ for a Woods-Saxon potential which fits Λ binding energies for $A \leq 89$.

^fDifference in half-value radius of the potential and the charge density.

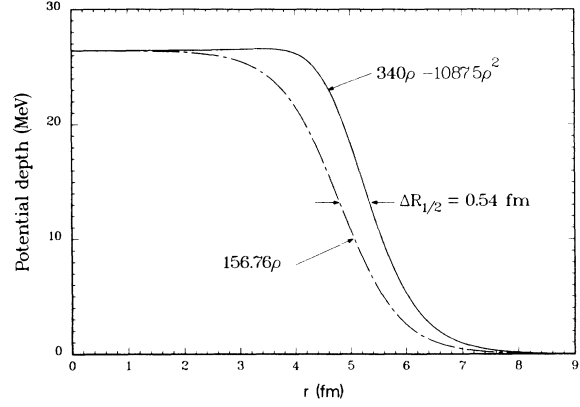


FIG. 2. Comparison of the shape (Fermi function) of $\rho(r)$ for $A = 89$ with the form $-V(r) = 56.67f(r) - 30.21f^2(r)$ in MeV obtained from the ρ^2 potential of Table II assuming $\rho_0 = \frac{1}{6} \text{ fm}^{-3}$. The important feature is the difference in the half-value radius of the two functions (cf. Ref. 19).

The ρ^2 term in Eq. (2) may arise from the density dependence of the ΛN interaction,²² as would be the case for Skyrme models,¹³ or from certain forms of $\Lambda N N$ three-body interactions,²³ or perhaps quark rearrangement effects.²⁴ This term need not be quadratic in form. The essential point is that a repulsive ρ^γ term, with $\gamma > 1$, leads to a potential with depth $V_1 - V_2$ and an increased central radius,¹⁹ a surface effect which is independent of A . This point is illustrated in Fig. 2. In fact, if $y = V_2 / (V_1 - V_2)$ and $\gamma = 2$, we have for the half-depth radius of the potential,

$$R_{1/2} = c + a \ln[y + (1 + y^2)^{1/2}], \quad (12)$$

so the increase in radius is, to a good approximation, linear in V_2 [$R_{1/2} = c + ay + O(y^3)$]. Clearly, a fixed increase in the radius increases the effective radius parameter r_0 , defining $R_{1/2}$, for light nuclei relative to r_0 for heavy nuclei, and as V_2 increases for fixed $V_1 - V_2$ there will be a value beyond which the effective radius parameter of the potential decreases with increasing A . In essence, this mechanism explains the difference in radii

TABLE II. Local, density-dependent potentials.

$-V(r)$	$B_{\Lambda}({}^{16}\text{O})^a$		$B_{\Lambda}({}^{89}\text{Y})^b$			
	s_{Λ}	p_{Λ}	s_{Λ}	p_{Λ}	d_{Λ}	f_{Λ}
$505.2\rho - 605.5\rho^{4/3}$	13.113	2.497	22.935	17.376	10.909	3.864
$387.0\rho - 738.8\rho^{5/3}$	13.131	2.500	21.906	16.693	10.504	3.636
$340.0\rho - 1087.5\rho^2$	13.127	2.498	21.445	16.420	10.367	3.579
$292.2\rho - 5300.0\rho^3$	13.106	2.500	20.158	15.674	9.988	3.415
$B_{\Lambda}(\text{expt})^c$	13.0	2.5	22.5	16.0	9.5	2.5

^a $3pF$ density (Ref. 15).

^b $2pF$ density; $r_0 = 1.08$ fm, $a = 0.54$ fm.

^cErrors are ± 1 MeV for ${}^{89}\text{Y}$ and ± 0.5 MeV for ${}^{16}\text{O}$; all entries in Table II are in MeV.

between the potential and the underlying density.

For the case $\gamma = 2$, the potential parameters in Table II imply $y \approx 1.12$ or a change in $R_{1/2}$ of about 0.5 fm. We contrast this with the very strong ρ^2 term in the Λ potential suggested by Bychkov.²⁵ In this case, “surface hyperon states” would exist, localized in the pocket of attraction produced at the nuclear surface. His choices²⁵ of V_1 and V_2 correspond to $y \approx 3.2$ – 4.9 , implying a change in $R_{1/2}$ of 1.0–1.25 fm. This is a much larger effect than we find; the potentials of Bychkov²⁵ are inconsistent with the level spacing in heavy hypernuclei (e.g., ${}^{89}\text{Y}$).

Giving the potential in terms of Fermi (Woods-Saxon) functions [Eq. (9)] is very useful for gaining analytic insights into the properties of the potential. However, to apply Eqs. (1)–(4), we use the empirical charge densities. This is a more satisfactory procedure, particularly for light nuclei where Fermi functions do not provide a good description of the charge densities and the charge radii show considerable deviation from a smooth behavior. For example, even though ${}^{16}\text{O}$ appears to fit well with the systematics exhibited for heavier nuclei in Table I, the use of a diffuseness $a = 0.54$ fm leads to too high a central density ρ_0 compared with the empirical value. Actually, it is the value of the density just inside the nuclear surface, before it begins to drop off rapidly, that is remarkably constant for all nuclei, while the central density may go up or down depending on orbit occupancies.

D. Fits to B_{Λ} with local potentials

As the size of a potential well is increased, the single-particle spectrum becomes more compressed. From the preceding subsection, we see that the size of the well can be controlled by the strength of the density-dependent terms. In order to study single-particle spectra as a function of A , it is sufficient to consider the binding energies of pairs of orbits in ${}^{16}\text{O}$ and ${}^{89}\text{Y}$. For example, we choose the s_{Λ} and p_{Λ} orbits in ${}^{16}\text{O}$ and the p_{Λ} and f_{Λ} orbits in ${}^{89}\text{Y}$ [the (π^+, K^+) data show a much more clearly defined peak corresponding to the p_{Λ} orbit than it does for the s_{Λ} ground state]. We take the experimental binding energies to be 13.0 and 2.5 MeV in ${}^{16}\text{O}$ and 16.0 and 2.5 MeV in ${}^{89}\text{Y}$. If these energies are fitted by a prescribed density

dependence, the systematic behavior of the binding energies shown in Fig. 1 ensures a reasonable fit to all measured binding energies.

We consider local potentials of the form

$$-V(r) = A\rho(r) - B\rho^{\gamma}(r) \quad (13)$$

with $\gamma = \frac{4}{3}, \frac{5}{3}, 2$, and 3. As a function of ρ , $V(r)$ turns over at a density given by $\rho_m = (A/B\gamma)^{1/(\gamma-1)}$. Note that as the repulsive term increases in strength ρ_m moves to smaller densities, and the potential can develop a pocket at the surface if $\rho_m < \rho_0$ because $V(\rho)$ will increase from $r = 0$ until the density drops below ρ_m . For the values of A and B which fit the two binding energies for ${}^{16}\text{O}$, ρ_m is close to the central density ρ_0 of nuclei. In fact, for $\gamma = 2$, $\rho_m \approx \rho_0$. This behavior, which is shown in Fig. 3, means that the interior potential depth is extremely stable from nucleus to nucleus. The interior density, itself, is rather constant, but small variations will be smoothed out in the potential. Table II gives the parameters which, for each type of density dependence, fit the binding energies in ${}^{16}\text{O}$. Also given are the binding ener-

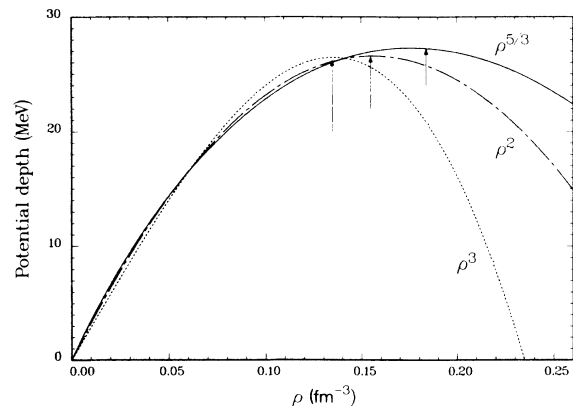


FIG. 3. Curves showing the “saturation” behavior of $V(\rho)$ and the position of ρ_m (arrows) relative to the interior density of nuclei ($\rho \sim 0.16$ – 0.175 fm $^{-3}$) for several of the potentials in Table II.

TABLE III. Parameters for nonlocal Λ -nucleus potentials.^a

Density dependence ρ^γ	\tilde{t}_0 (MeV fm ³)	t_3 (MeV fm ^{3\gamma})	$t_1 + t_2$ (MeV fm ⁵)	m^*/m^b	D_Λ^c (MeV)
ρ^2	-402.6	3394.6	103.44	0.80	27.5
	-404.0	3300.0	120.0	0.775	27.9
$\rho^{5/3}$	-456.0	2306.0	103.44	0.80	27.7
$\rho^{4/3}$	-659.0	2200.0	130.0	0.76	28.1

^aParametrization of Eqs. (1)–(4).

^bEvaluated at center of $^{89}\Lambda\text{Y}$ for $2pF$ density with $\rho_0=0.1685\text{ fm}^{-3}$ ($r_0=1.08\text{ fm}$, $a=0.54\text{ fm}$), using Eq. (4).

^c $D_\Lambda = -U(0)$, Eq. (2), $\rho \rightarrow \rho_0=0.157$ for $r_0(A=\infty)=1.15\text{ fm}$.

gies for $^{89}\Lambda\text{Y}$ obtained with each of the potentials. The overbinding of the f orbit is a consistent feature of the potentials fitted to $^{16}\Lambda\text{O}$. Corresponding discrepancies occur for the $^{16}\Lambda\text{O}$ spectrum if the $^{89}\Lambda\text{Y}$ spectrum is fitted. The fact that $^{16}\Lambda\text{O}$ and $^{89}\Lambda\text{Y}$ cannot be fitted simultaneously with a local potential based on the empirical charge densities is related to the fact that the $\Delta R_{1/2}$ values, listed in the last row of Table I, are not constant as a function of A , in contrast to the behavior suggested by Eq. (12). Nevertheless, a local density-dependent interaction almost succeeds in reproducing the data. Ahmad, Mian, and Rahman Kahn²⁶ have obtained a potential with $\gamma = \frac{5}{3}$ by fitting to ground-state binding energies of light hypernuclei which is almost identical to the corresponding potential listed in Table II. Their set B solution has $-V(r)=384.0\rho - 714.2\rho^{5/3}$.

E. Fits to B_Λ with nonlocal potentials

If we take the model prescribed by Eqs. (1)–(4) seriously, we have one more significant parameter left to vary, namely, the effective mass $m^*(r)$. Since the energy levels

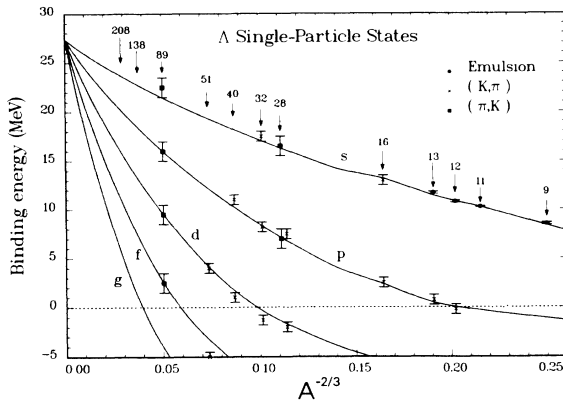


FIG. 4. The data on binding energies of Λ single-particle states (see caption to Fig. 1) compared to the binding energies obtained for the first of the density-dependent, nonlocal potentials in Table III with ρ^2 density dependence. For $A > 16$, the density is obtained from a Fermi function with $r_0=1.144 - 1.276 A^{-2/3}\text{ fm}$ and $a=0.54\text{ fm}$ (cf. the fourth row of Table I). For $A \leq 16$, empirical charge densities from Ref. 15 are used. The use of empirical charge densities leads to the kinks seen in the binding-energy curves for small A .

in a nonlocal potential are spread out by the energy-dependent term in the equivalent local potential of Eq. (1), it is easy to see that a simultaneous description of the binding energies in $^{16}\Lambda\text{O}$ and $^{89}\Lambda\text{Y}$ is likely to be achievable. The density dependence (t_3) can be used to adjust the radius of the well to fit $^{16}\Lambda\text{O}$ while the effective mass can be used to counteract the compression of the $^{89}\Lambda\text{Y}$ spectrum evident in Table II. A series of potentials, which all give excellent fits to the data in Fig. 1, are listed in Table III. The values of $t_1 + t_2$ correspond to $m^*/m \approx 0.8$ in the interior of the hypernucleus. It is important that realistic densities be used since the connection between m^*/m and ρ_0 in Eq. (4) strongly affects the local well depth in Eq. (1). For different empirical charge densities fitted to electron scattering data, the differences in Λ binding energies are minimal ($< 200\text{ keV}$). For each type of density dependence ($\gamma = \frac{4}{3}$, $\frac{5}{3}$, or 2) an essentially identical fit, with roughly the same m^*/m and D_Λ , can be obtained. The interplay between the ρ and ρ^γ terms simply gives potential wells of the correct depth and size to fit the data. The binding energies are relatively insensitive to the finer details of the radial shape. This can be seen from Figs. 4 and 5, where the binding energies for potentials with ρ^2 and $\rho^{4/3}$ density dependence, respectively, are compared with the data. In summary, the well depth, the well radius, and m^*/m are rather tightly constrained by data.

It can be seen from Fig. 1 that an excellent fit to the

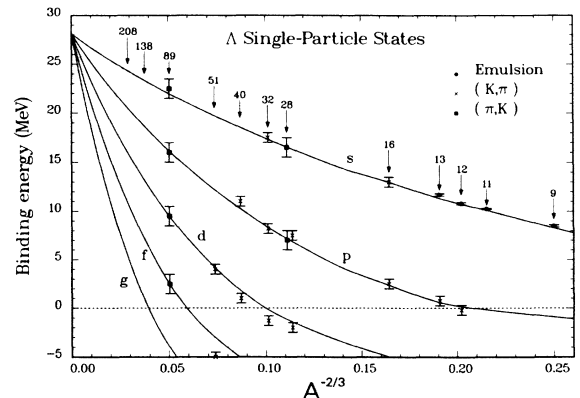


FIG. 5. Same as Fig. 4 but for the potential in Table III with $\rho^{4/3}$ density dependence.

binding energies can be obtained with a simple Woods-Saxon potential with a depth of 28 MeV and a radius parameter $r_0 = 1.128 + 0.439 A^{-2/3}$ which decreases slowly with increasing A . From a practical point of view, this potential is as good as any for predicting Λ binding energies.

III. COMPARISON WITH NUCLEON-NUCLEUS POTENTIALS

As we have, in fact, assumed, a useful representation of the NN or ΛN effective interaction v_{eff}^i , with $i = \Lambda$ or N , in the nucleus is provided by the Skyrme²⁷ ansatz $v_{\text{eff}}^i = v_2^i + v_3^i$, with

$$\begin{aligned} v_2^i(\mathbf{r}-\mathbf{r}') &= t_0^i(1+x_0^i P_\sigma)\delta(\mathbf{r}-\mathbf{r}') \\ &+ \frac{1}{2}t_1^i[k'^2\delta(\mathbf{r}-\mathbf{r}') + \delta(\mathbf{r}-\mathbf{r}')k^2] \\ &+ t_2^i\mathbf{k}'\cdot\delta(\mathbf{r}-\mathbf{r}')\mathbf{k}, \\ v_3^i(\mathbf{r}_1, \mathbf{r}_2, \mathbf{r}_3) &= t_3^i\delta(\mathbf{r}_1-\mathbf{r}_2)\delta(\mathbf{r}_2-\mathbf{r}_3), \end{aligned} \quad (14)$$

where $\mathbf{k} = (\nabla_{\mathbf{r}} - \nabla_{\mathbf{r}'})/2i$ and $P_\sigma = \frac{1}{2}(1 + \sigma_1 \cdot \sigma_2)$. The parameters t_0^i and t_1^i correspond to the interaction in two-body s states, while the t_2^i term operates in relative p states. The interaction v_3^i need not be considered as a genuine three-body force, but rather as a means of simulating the density dependence of the effective interaction. The Skyrme model has been extensively applied to nucleon bound-state spectra by the Orsay group^{16,28} and to Λ hypernuclei by Rayet.^{13,17} Negele and Vautherin²⁹ have attempted to calculate the parameters t_i^N from realistic NN potentials, with some success.

For an interaction of the form in Eq. (14), the self-consistent potential $U_i(r)$, $i = \Lambda$ or N , can be written in the approximate form [assuming $\rho_n = \rho_p$, and omitting spin-orbit terms, Coulomb terms, and terms involving derivatives of $\rho(r)$]

$$\begin{aligned} U_i(r) &= U_i^H(r) - U_i^F(r), \\ U_i^H(r) &= t_0^i \left[1 + \frac{x_0^i}{2} \right] \rho(r) + \frac{1}{4}t_3^i \left[1 + \frac{\delta_{i,\Lambda}}{2} \right] \rho^2(r) \\ &+ \frac{1}{4}(t_1^i + t_2^i)T(r), \\ U_i^F(r) &= \frac{\delta_{i,N}}{4} [t_0^N(1+2x_0^N)\rho(r) + \frac{1}{4}t_3^N\rho^2(r) \\ &+ \frac{1}{4}(t_1^N - t_2^N)T(r)], \end{aligned} \quad (15)$$

where U_i^H is the Hartree term, U_i^F is the Fock exchange term, which is absent for the Λ [cf. Eq. (2)], and $T(r)$ is given by Eq. (3) in the Thomas-Fermi approximation. The energy eigenvalues and wave functions can be obtained¹⁴ from the solution of an ordinary Schrödinger equation with an equivalent local potential given by Eq. (1), plus some small corrections involving derivatives of $m_i^*(r)/m$, where [cf. Eq. (4)]

$$\frac{\hbar^2}{2m_i^*(r)} = \frac{\hbar^2}{2m_i} + \frac{1}{4}(t_1^i + t_2^i)\rho(r) + \frac{1}{16}\delta_{i,N}(t_2^N - t_1^N)\rho(r). \quad (16)$$

The nonlocality of the Skyrme interaction, i.e., the terms involving t_1 and t_2 , has been eliminated in favor of an energy-dependent potential $V_i(r, E)$. The parameters for a representative selection of NN and ΛN models, taken from the work of Beiner *et al.*,²⁸ Rayet,¹³ and this work, are given in Table IV.

Now consider some qualitative features of Skyrme models for nucleon orbits. First of all, a substantial contribution from the $t_3^N\rho^2(r)$ term in $U_N(r)$ is required to account for the observed level density in nuclei. If $t_3^N = 0$, the nucleon orbits are far too spread out in energy. A variety of models are discussed by Beiner *et al.*²⁸ For instance, their model SVI has a large t_3^N , which serves to compress the levels near the Fermi surface, in agreement with the data. This model has $m^*/m \approx 0.94$ in the nuclear interior, i.e., only a modest degree of nonlocality. Model SVI, however, produces too little binding for deeply bound levels. For example, in ¹⁶O, one finds 27

TABLE IV. Parameters^a of Skyrme models for NN and ΛN interactions.

Model	\tilde{t}_0 (MeV fm ³)	t_1 (MeV fm ⁵)	t_2 (MeV fm ⁵)	t_3 (MeV fm ⁶)	m^*/m
SVI ^b	-1423	272	-138	17000	0.94
SII ^b	-1369	587	-27	9331	0.55
11 ^c	-303	0	0	2000	1.0
2 ^c	-568	162	-39	6074	0.77
d	-340	0	0	2900	1.0
e	-403	103	0	3395	0.80

^aNote that $\tilde{t}_0 = t_0(1+x_0/2)$; SVI and SII refer to the NN case, the other rows to ΛN . Effective masses are evaluated from Eq. (16) with $\rho_0 = 0.1685 \text{ fm}^{-3}$ (cf. Table III).

^bReference 28.

^cReference 13.

^dThis work; ρ^2 potential of Table II.

^eThis work, first potential in Table III. Only the sum $t_1 + t_2$ enters; it is given in the column for t_1 .

MeV for the 0s proton binding energy, as compared to the experimental value³⁰ of 44 ± 7 MeV from the $(e, e'p)$ reaction. Model SII, on the other hand, which has $m^*/m = 0.55$, gives much better results for the deep levels (the 0s in ^{16}O is now bound by 38 MeV), but too low a level density near the Fermi surface. Within the Skyrme model, it is not possible to simultaneously describe the nucleon level density at the Fermi surface (which requires $m^*/m \approx 1$) and the deeply bound levels (which need $m^*/m \approx \frac{1}{2}$). In contrast, for the more weakly interacting, distinguishable Λ , an excellent description of the binding energies, from the most deeply bound to unbound resonances, is possible with a single value of m^*/m .

For a Gaussian two-body interaction with no space-exchange (P_X) component and range $1/\mu$, we expect

$$\frac{t_1 - t_2}{\tilde{t}_0} = -\frac{1}{\mu^2}, \quad t_1 + t_2 = 0, \quad (17)$$

where $\tilde{t}_0 = t_0(1 + x_0/2)$. For the SII parameters of Table IV, we find $(t_1 - t_2)/\tilde{t}_0 = -0.45$ or $\mu \approx 295$ MeV, larger, though not overwhelmingly so, than the pion mass. (We note that the pion contributes substantially to the Fock potential due to exchange even in spin-isospin saturated nuclei.) The equality $t_1 = -t_2$ is strongly violated, indicating the presence of strong P_X forces for the NN case, as expected theoretically.²⁹ For the ΛN case, we anticipate a smaller range $1/\mu$, since one-pion exchange does not contribute to the $\Lambda N \rightarrow \Lambda N$ potential. Some degree of P_X dependence is expected from K and K^* exchanges,³¹ but less than for NN . Thus, we expect both $(t_1^\Lambda - t_2^\Lambda)/\tilde{t}_0$ and $t_1^\Lambda + t_2^\Lambda$ to be smaller than their counterparts for the N case. As a consequence, we expect that m^*/m will not differ greatly from unity.

What about the choices of \tilde{t}_0^Λ and t_3^Λ ? Calculations based on one-boson exchange models provide an estimate for \tilde{t}_0^Λ , i.e., the term in the potential which is linear in the density. One finds³¹ well depths of 56 MeV for Nijmegen³² model D and 50 MeV for model F , to be identified with $\rho_0 \tilde{t}_0^\Lambda$, where $\rho_0 \approx \frac{1}{6} \text{ fm}^{-3}$. This gives the estimate $\tilde{t}_0^\Lambda \approx -300$ to -330 MeV, consistent with model 11 of Rayet¹³ and our own local model. By itself, the term $\tilde{t}_0^\Lambda \rho(r)$ leads to the well-known "overbinding" problem. The necessary additional repulsion is provided by the term $t_3^\Lambda \rho^2(r)$. As explained in Sec. II B, this term increases the effective radius of the potential well, giving a compression of the single-particle spectrum. For both nuclei and hypernuclei, a substantial ρ^2 term is required.

It is also interesting to compare our results with an interpretation of the binding energies of Λ hypernuclei in terms of phenomenological ΛN and ΛNN forces. A satisfactory description of the binding energies of the s -shell hypernuclei, $^9_\Lambda\text{Be}$, $^{13}_\Lambda\text{C}$, and the Λ well depth is obtained by Bodmer and Usmani²³ using ΛN interactions which fit Λp scattering data and strongly repulsive ΛNN interactions which contribute -25 to -30 MeV to D_Λ . These repulsive ΛNN contributions are of the same size as the contributions from the ρ^2 terms of the phenomenological single-particle potentials listed in Tables II and III.

The discussion thus far has not made reference to the role of quarks. The differences between the Λ and N

spectra hinge on several factors.

(1) The nonlocality of the self-consistent field (i.e., the choice of t_1 and t_2). The differences between Λ and N largely reflect the range of the effective interaction, which is larger for NN than for ΛN because of the role of π exchange for the former. This is a nonperturbative long-range effect having nothing to do with short-range quark properties.

(2) The role of $t_3 \rho^2(r)$ terms. These are a complicated mixture of density-dependent modifications of the two-body interaction and perhaps genuine three-body interactions. It has been proposed that the "Pauli pressure" due to quark antisymmetrization^{24,33} generates an effective ΛNN force. Effects of partial deconfinement of strange quarks³⁴ in the nucleus, or the possibility of an increased size for hyperons³⁵ relative to nucleons (even in free space) are intriguing, but the fact that the B_Λ data, when fitted by a potential, are insensitive to the precise form of the density dependence makes it impossible to relate behavior of the B_Λ values to any specific source such as quark degrees of freedom. The level spectra are consistent with the picture of the Λ as a distinguishable baryon.

(3) The role of Fock terms for the nucleon. These are important in a quantitative study, but the main feature of SII, which reproduces deeply bound N levels, is that $m^*/m \approx \frac{1}{2}$ in the nuclear interior, and this is true already in the Hartree approximation, i.e.,

$$\frac{m^*}{m} = \begin{cases} 0.55 & \text{Hartree-Fock} \\ 0.47 & \text{Hartree} \end{cases}$$

The Fock terms tend to reduce the size of the Perey effect, i.e., the damping of the wave function in the nuclear interior. Thus, the principal differences between Λ and N spectra are due to different ranges (t_1, t_2) and three-body terms (t_3), not to the presence of a Fock term for the nucleon.

IV. DISCUSSION

The parameter sets in Table III represent the end product of our fit to the Λ binding-energy data from in-flight (π^+, K^+) and (K^-, π^-) reactions and emulsion experiments. The fit is made with a density-dependent and non-local Λ -nucleus potential of a form suggested by Rayet's Skyrme Hartree-Fock calculations.¹³ Derivatives of the density, which appear in the Skyrme Hartree-Fock formulation to take into account some aspects of the finite range of the ΛN interaction, have been omitted on the grounds that finite-range effects are included in an approximate way by the use of empirical charge densities. We have experimented with including the derivative terms which appear in Rayet's formulation, but they give rise to rather unphysical "glitches" in the surface region of the Λ -nucleus potential, at least in our non-self-consistent approach. Three parameters are needed to give a good fit to the data. The interplay between terms with different powers of the density simply ensures that wells have the correct depth (essentially constant) and size as a function of mass number. The effective-mass term spreads out the spectrum (for $m^*/m < 1$) and pro-

duces the correct level density for light and medium-heavy nuclei. The exact form of the density dependence is unimportant, but once chosen the parameters \tilde{t}_0 , t_3 , and $t_1 + t_2$ are rather tightly constrained by the data. As a caveat, we note that the most recent (π^+ , K^+) data¹ is still under analysis³ and that our assignment of errors to the Λ binding energies is somewhat arbitrary. However, there is good agreement, not shown in Fig. 1, between the Λ binding energies extracted from different sets of experimental data. Consequently, we do not anticipate any significant changes to the overall picture presented in Fig. 1.

Recently, a number of attempts have been made to calculate Λ -nucleus potentials starting from a free ΛN interaction (for earlier work see Ref. 31). A G matrix is calculated for nuclear matter as a function of density and is then parametrized for use in constructing a Λ -nucleus potential, e.g., by folding. The G matrices of Yamamoto and Bando²² are obtained using the Nijmegen interaction.³² The Λ well depth that results is consistent with the empirical value, and the effective mass, which arises from exchange forces and short-range correlations due to hard cores, takes a value $m^*/m \sim 0.78$. Refinements in the construction of Λ -nucleus potentials have subsequently been made by Yamamoto³⁶ and by Kohno.³⁷ These potentials are quite successful in predicting Λ single-particle binding energies. Direct comparisons with our empirical potential are not easy to make because the density dependence, which can take a variety of forms, differs from case to case. However, Kohno³⁷ does display equivalent local potentials which could be compared with our results. Work has also been done by a Jülich group,³⁸ who start with the generalized Bonn potential.³⁹ They obtain $m^*/m = 0.87$ and a well depth of 28.5 MeV. Thus, the general features of the Λ -nucleus potential obtained from

the free ΛN interaction seem to be consistent with those we have obtained from a rather precise fit to the binding energies of Λ single-particle levels.

The Λ binding energies shown in Fig. 1 provide a "textbook" example of single-particle structure in nuclear physics. In ordinary nuclei, single-particle strength rapidly becomes fragmented with increasing excitation energy, and the deeply bound hole states become so broad as to be essentially unobservable. Even in the region of the Fermi surface, where excellent examples of the basic single-particle structure abound, coupling to vibrational states of the core is important and leads to an apparent compression of the single-particle spectrum. In the hypernuclear case, the fact that the Λ is a distinguishable particle, which interacts rather weakly with the nuclear core, leads to a clearly defined set of single-particle states. These states can be thought of as doorway states which acquire a spreading width by mixing with a dense background of hypernuclear levels. An estimation of these widths, together with escape widths (e.g., for proton emission) is necessary to understand the widths of the peaks observed in the (π^+ , K^+) reaction on heavy targets.^{40,41} The observed peaks are certainly broader than the experimental resolution. The widths of the peaks will limit the largest mass number for which the Λ single-particle structure can be investigated, at least with the present resolution of about 3 MeV, since the intershell spacing will eventually become comparable with the width. However, it should be possible to investigate the structure ($h_{11/2}^{-1} I_{\Lambda}$) for a ¹³⁸Ba target.

This work has been supported in part by the U.S.-Israel Binational Science Foundation and in part by Contract No. DE-AC02-76CH00016 with the U.S. Department of Energy.

¹R. Chrien, Proceedings of XIth International Conference on Particles and Nuclei, Kyoto, 1987 [Nucl. Phys. **A478**, 705c (1988)].
²D. J. Millener, A. Gal, C. B. Dover, and R. H. Dalitz, Phys. Rev. C **31**, 499 (1985).
³R. Chrien (private communication).
⁴C. Milner *et al.*, Phys. Rev. Lett. **54**, 1237 (1985).
⁵M. Juric *et al.*, Nucl. Phys. **B52**, 1 (1973); T. Cantwell *et al.*, *ibid.* **A236**, 445 (1974).
⁶J. Lemonne *et al.*, Phys. Lett. **18**, 354 (1965).
⁷R. H. Dalitz, in *Nuclear Physics*, edited by C. DeWitt and V. Gillet (Gordon and Breach, New York, 1969), p. 701.
⁸R. Bertini *et al.*, Phys. Lett. **83B**, 306 (1979).
⁹R. Bertini *et al.*, Nucl. Phys. **A360**, 315 (1981).
¹⁰A. Bouyssy and J. Hüfner, Phys. Lett. **64B**, 276 (1976); A. Bouyssy, *ibid.* **84B**, 41 (1979).
¹¹A. Gal, in *Advances in Nuclear Physics*, edited by M. Baranger and E. Vogt (Plenum, New York, 1975), Vol. 8, p. 1.
¹²C. B. Dover, in *Proceedings of the International Symposium on Medium Energy Physics, Beijing, 1987*, edited by Chian Huan-Ching and Zheng Lin-Sheng (World Scientific, Singapore, 1987), p. 257.
¹³M. Rayet, Nucl. Phys. **A367**, 381 (1981).
¹⁴C. B. Dover and N. van Giai, Nucl. Phys. **A190**, 373 (1972).

¹⁵H. de Vries, C. W. de Jager, and C. de Vries, At. Data Nucl. Data Tables **36**, 495 (1987).
¹⁶D. Vautherin and D. M. Brink, Phys. Rev. C **5**, 626 (1972).
¹⁷M. Rayet, Ann. Phys. (N.Y.) **102**, 226 (1976).
¹⁸C. B. Dover, L. Ludeking, and G. E. Walker, Phys. Rev. C **22**, 2073 (1980).
¹⁹W. D. Myers, Nucl. Phys. **A204**, 465 (1973).
²⁰C. J. Batty, A. Gal, and G. Toker, Nucl. Phys. **A402**, 349 (1983).
²¹J. Friedrich and N. Voegler, Nucl. Phys. **A373**, 192 (1982).
²²Y. Yamamoto and H. Bando, Prog. Theor. Phys. Suppl. **81**, 9 (1985); Prog. Theor. Phys. **73**, 905 (1985).
²³A. R. Bodmer and Q. N. Usmani, Nucl. Phys. **A477**, 621 (1988).
²⁴S. Takeuchi and K. Shimizu, Phys. Lett. B **179**, 197 (1986).
²⁵A. S. Bychkov, Yad. Fiz. **40**, 408 (1984) [Sov. J. Nucl. Phys. **40**, 259 (1984)].
²⁶I. Ahmad, M. Mian, and M. Z. Rahman Khan, Phys. Rev. C **31**, 1590 (1985); M. Mian, *ibid.* **35**, 1463 (1987).
²⁷T. H. R. Skyrme, Nucl. Phys. **9**, 615 (1959).
²⁸M. Beiner, H. Flocard, N. van Giai, and P. Quentin, Nucl. Phys. **A238**, 29 (1975).
²⁹J. W. Negele and D. Vautherin, Phys. Rev. C **5**, 1472 (1972).
³⁰S. Frullani and J. Mougey, in *Advances in Nuclear Physics*,

- edited by J. W. Negele and E. Vogt (Plenum, New York, 1983), Vol. 14, p. 1.
- ³¹C. B. Dover and A. Gal, *Prog. Part. Nucl. Phys.* **12**, 171 (1984).
- ³²M. M. Nagels, T. A. Rijken, and J. J. de Swart, *Phys. Rev. D* **12**, 744 (1975); **15**, 2547 (1977); **20**, 1633 (1979).
- ³³E. V. Hungerford and L. C. Biedenharn, *Phys. Lett.* **142B**, 232 (1984).
- ³⁴T. Goldman, in *Intersections Between Particle and Nuclear Physics (Steamboat Springs, Colorado)*, Proceedings of the Conference on the Intersections of Particle and Nuclear Physics, AIP Conf. Proc. No. 123, edited by R. E. Mischke (AIP, New York, 1984), p. 799.
- ³⁵H. Nadeau, M. A. Nowak, M. Rho, and V. Vento, *Phys. Rev. Lett.* **57**, 2127 (1986).
- ³⁶Y. Yamamoto, *Prog. Theor. Phys.* **75**, 639 (1986).
- ³⁷M. Kohno, *Prog. Theor. Phys.* **78**, 123 (1987).
- ³⁸R. Büttgen, K. Holinde, B. Holzenkamp, and J. Speth, in *Intersections Between Particle and Nuclear Physics (Lake Louise, 1986)*, Proceedings of the Second Conference on the Intersections of Particle and Nuclear Physics, AIP Conf. Proc. No. 150, edited by D. F. Geesaman (AIP, New York, 1986), p. 924.
- ³⁹K. Holinde, *Nucl. Phys.* **A479**, 197c (1988).
- ⁴⁰A. Likar, M. Rosina, and B. Povh, *Z. Phys. A* **324**, 35 (1986).
- ⁴¹H. Bando, T. Motoba, and Y. Yamamoto, *Phys. Rev. C* **31**, 265 (1985).